FEMS Microbes, 2026, **7**, xtag042
https://doi.org/10.1093/femsmc/xtag042
Published: 23 July 2026
Research article – Microbes and Environment

Is a constitutive red-shift an advantage for oxygenic photosynthesis under M dwarf starlight? Insights from *Acaryochloris marina* sp. str. Moss Beach

Elisabetta Liistro [1,*], Beatrice Boccia [1], Mary Niki Parenteau [2], Nancy Y. Kiang [3], Nicoletta La Rocca [1,*]

[1]Department of Biology, University of Padova, Padova, 35131, Italy
[2]NASA Ames Research Center, Moffett Field, CA 94035, United States
[3]NASA Goddard Institute for Space Studies, New York, NY 10025, United States
*Corresponding authors. Elisabetta Liistro, Dipartimento di Biologia, Università di Padova, via U. Bassi 58b, Padova, 35131, Italy.
E-mail: elisabetta.liistro@phd.unipd.it; Nicoletta La Rocca, Dipartimento di Biologia, Università di Padova, via U. Bassi 58b, Padova, 35131, Italy.
E-mail: nicoletta.larocca@unipd.it.
Editor: Jana Jass

Abstract

In the next decades, space telescope missions will search for life evidence on exoplanets, focusing on robust biosignatures associated with oxygenic photosynthesis, including atmospheric oxygen accumulation and the Vegetation Red-Edge in surface reflectance spectra. Many habitable rocky exoplanets orbit M dwarf stars, whose spectral energy distribution may condition the rise and evolution of oxygenic photosynthesis. M dwarf stars emit predominantly far-red (700–750 nm) and near-infrared (750–1000 nm) light, and relatively little visible (400–700 nm) radiation, which on Earth predominantly drives photochemistry in most oxygenic phototrophs. Previous experiments proved some oxygenic phototrophs can photosynthesize under simulated M dwarf light but less efficiently than under solar radiation simulated in the range 365–780 nm. Indeed, tested organisms present photosynthetic apparatus evolved to harvest Sun's visible light, however, M dwarfs' irradiation might select adaptations optimized for harvesting far-red/near-infrared light. We measured sensitivities of a far-red/near-infrared-utilizing cyanobacterium, *Acaryochloris marina* sp. str. Moss Beach to simulated M dwarf spectrum and primeval anoxic, CO_2-rich atmosphere. This strain constitutively presents a high content of chlorophyll *d*, with *in vivo* absorption peak at 710 nm. Its permanently red-shifted photosynthetic apparatus required no acclimation to the stellar spectrum, maintaining strong growth and oxygen production, higher than that registered under simulated solar light. Moreover, abundant chlorophyll *d* caused a shift in whole-cell reflectance: the red-edge was beyond 700 nm, resulting in a *Chl* d-*near-infrared-edge*. Overall, a potentially similar metabolism on exoplanets orbiting M dwarfs could successfully produce both a gaseous biosignature and a characteristic surface biosignature.

Keywords far-red light, photosynthesis, astrobiology, M-dwarf stars, biosignature, Acaryochloris marina

Introduction

In the last 20 years, space missions such as Kepler, the Transiting Exoplanet Survey Satellite (TESS, NASA) and the Global Astrometric Interferometer for Astrophysics (GAIA, ESA), have discovered a large number of exoplanets, over 6000 at the time of writing (From www.exoplanets.nasa.gov consulted on April 8, 2025). Some of these planets have been recognized as potentially habitable as their features and those of their host star(s) may support the presence and evolution of life (Kasting et al. 1993, Kaltenegger 2017, Méndez et al. 2021). Among these, rocky Earth-like exoplanets were found to be common around M dwarf stars (Kopparapu et al. 2013, Hsu et al. 2020). These stars, also referred to as M stars or red dwarfs, are considered viable targets for the search for life as not only do they frequently host rocky planets but they also have a lifespan long enough to allow for a biosphere to evolve (Shields et al. 2016). Moreover, their strong early stellar activity is considered to decline to solar levels within ∼3 billion years, thus not precluding habitability (Gale and Wandel 2016, O'Malley-James and Kaltenegger 2017, Schwieterman et al. 2018).

In the search for life on planets orbiting M dwarf stars, *in situ* detection is not feasible, as the closest M dwarf, Proxima Centauri b, is 4.2 light-years from Earth (Anglada-Escudé et al. 2016). Life detection must thus rely on remote sensing of *biosignatures*: patterns or molecules of unequivocal biological origin (Schwieterman et al. 2018, Claudi and Alei 2019). Missions such as the Atmospheric Remote-Sensing Infrared Exoplanet Large-survey (ARIEL, ESA) and the Habitable Worlds Observatory (HWO, NASA) will be launched

Received: 10 April 2026. **Revised:** 26 June 2026. **Accepted:** 7 July 2026

in the coming years with the purpose of characterizing exoplanets atmospheres, looking for biosignatures (Tinetti et al. 2018, Feinberg et al. 2026). One of the strongest remotely detectable biosignatures on our planet is the presence of oxygen, O_2, and its byproduct ozone, O_3, in a planet's atmosphere (Schwieterman et al. 2018, Cavalazzi and Westall 2019, Claudi and Alei 2019). Since on Earth the abundance of these molecules is caused by oxygenic photosynthesis, the metabolic process operated by cyanobacteria, algae, and plants (Cavalazzi and Westall 2019), scientists have been discussing on the feasibility of this metabolisms around M dwarf stars (Tinetti et al. 2006, Kiang et al. 2007a,b).

M dwarfs are cold and faint stars that emit mainly far-red (FR, 700–750 nm) and near-infrared (NIR, 750–1000 nm) light, and very low visible (VIS, 400–700 nm), in contrast to G stars, like the Sun (Chabrier et al. 1996, Pecaut and Mamajek 2013), whose emission is stronger in the visible. This emission spectrum challenges the possibility of canonical oxygenic photosynthesis to have evolved around such planets as this process on Earth relies mainly on VIS light, which is preferentially harvested by most common pigments and antenna complexes. Nonetheless, models indicate that the small amount of VIS light reaching a planet orbiting an M dwarf star could still allow for oxygenic photosynthesis to work efficiently, with a productivity estimated to be up to the 22% of that on Earth (Gale and Wandel 2016, Ritchie et al. 2018, Gray et al. 2025). If photosynthetic adaptations such as three or four photosystems in series have evolved around M dwarf stars, the productivity of oxygenic photosynthesis has been estimated to potentially increase to over the 75% of Earth's (Kiang et al. 2007b). Additionally, oxygenic photosynthetic organisms generate another biosignature that is among the most studied: the Vegetation Red-Edge, VRE. VRE is a sharp increase in reflectance around 700 nm toward the NIR, as a consequence of the contrast between the high absorption in the visible, due to chlorophyll molecules, and the scattering of NIR due to cell structures (Gausman et al. 1975, Tucker et al. 1985, Grant 1987, Sagan et al. 1993, Turnbull et al. 2006, O'Malley-James and Kaltenegger 2018). It was proposed that, around an M dwarf, this feature of (eventual) oxygenic phototrophs could be altered because of the need to harvest longer wavelengths (Wolstencroft and Raven 2002). Due to the presence of FR or near-infra-red (NIR) harvesting pigments, the VRE might be shifted and become a "NIR" edge (Tinetti et al. 2006, Kiang et al. 2007a).

Recently, it was experimentally demonstrated that oxygenic photosynthesis and growth is possible under a simulated M dwarf spectrum in several Earth organisms, with different efficiencies (Boccia et al. 2026, Liistro et al. 2024, Battistuzzi et al. 2023a, 2023b). Cyanobacteria are ideal targets for these studies, as in recent decades some strains were found capable of photosynthesizing not only with visible light but also with solely FR light via the Far-Red Light Photoacclimation (FaRLiP) (Gan et al. 2014). In these species, the FaRLiP response is enabled by the presence of a specific gene cluster expressed in FR light which leads to the synthesis of (i) red-shifted pigments (chlorophyll *d*, Chl *d*, and chlorophyll *f*, Chl *f*), (ii) allophycocyanin proteins with red-shifted chromophores (far-red allophycocyanin, FR-APC), (iii) paralog subunits of photosystems that incorporate the pigments. With this remodeling of the photosynthetic apparatus, organisms present a shoulder of absorption in the FR and fluorescence emission shifted to longer wavelengths (Gan et al. 2014, Ho, Soulier, et al. 2017). *Chlorogleopsis fritschii* PCC6912 acclimated to the simulated M dwarf spectrum showed the activation of FaRLiP, leading to the use of both the visible and FR light available in a simulated stellar spectrum (Battistuzzi et al. 2023a).

These results are fundamental to understand the limits of oxygenic photosynthesis around M dwarfs, however, they all consider organisms evolved for photosynthesizing with visible light and that canonically harbor VIS photosystems, with some exception of strains that at most can acclimate to increase their FR absorption capacity through uphill energy transfer (Elias et al. 2024). It was hypothesized that the eventual evolution of oxygenic phototrophs under the irradiance of M dwarfs could have selected particular adaptations such as red-shifted pigments, modified antennae, or a higher number of photosystems working in series (Kiang et al. 2007a,b; Takizawa et al. 2017, Chitnavis et al. 2024).

Curiously, on Earth we have examples of organisms, adapted to FR-enriched light niches, with a unique photosynthetic apparatus that has constitutive and strongly red-shifted absorbance, namely in the cyanobacterial strains of the species *Acaryochloris marina* (Miyashita et al. 1996, Larkum and Kühl 2005). *A. marina* strains are characterized by the permanent large presence of Chl *d* in Photosystem I & II, accounting for more than 90% of the total chlorophyll content, and participating both in light harvesting and charge separation, with maximum absorption at 740 nm (Chen et al. 2002, Badshah et al. 2017). It is also interesting to notice how ancestral the divergence of this genus is in the evolution of oxygenic photosynthesis: the split of the *Acaryochloris* genus from the cyanobacterial species tree was found to precede the appearance of the FaRLiP phenotype, dated in the Paleoproterozoic (Antonaru et al. 2025).

When considering the eventual evolution of oxygenic photosynthesis around M dwarfs, *A. marina* is an excellent example of the evolution of a photosynthetic apparatus that mainly harvests FR wavelengths.

In this work, we evaluated the response of a strain of *Acaryochloris marina* to simulated light and atmospheric conditions. Experiments were designed to characterize basic ecophysiology of this strain, to distinguish whether this strain acclimates to a change in light spectra between FR and solar light, and to quantify its activity under simulated M dwarf light in an anoxic Archean-like atmosphere as a potential scenario for far-red photosynthesis as an early metabolism on a planet around an M dwarf.

Materials and methods

Tested organism and experimental plan

The organism tested in this study was *Acaryochloris marina* sp. str. Moss Beach. *A. marina* sp. str. Moss Beach was found as an epiphyte of a brown macroalga, in the rocky intertidal zone of the J.V. Fitzgerald Marine Reserve, California, and the Chl *d* in its photosynthetic apparatus can reach up to 99% of the total chlorophyll content (Kiang et al. 2022). Due to its Chl *d*-bearing photosystems, the *in vivo* Q_y absorption peak of *A. marina* sp. str. Moss Beach is at 705 nm, with its tail arriving at 750 nm. This strain lacks the accessory pigments phycobiliproteins, hence the light harvesting is only operated with chlorophylls and marginally with carotenoids, similarly to other strains of *A. marina*, as *A. marina* CCMEE 5410 and *A. marina* HICR111A (Chan et al. 2007, Mohr et al. 2010, Kiang et al. 2022).

As this strain is of recent discovery, we first identified the medium, temperature and light intensity suitable for the simulations. We then assessed whether *A. marina* sp. str. Moss Beach performed a physiological acclimation to a simulated M-dwarf spectrum, comparing the response with cells exposed to solely FR light and solar light. Finally, we proceeded by investigating its performances in simulated planetary conditions combining irradiation with a simulated anoxic primeval atmosphere.

Cultivation conditions for preliminary physiological sensitivity experiments

We obtained the initial inoculum of *Acaryochloris marina* sp. str. Moss Beach, isolated at Moss Beach, in the J.V. Fitzgerald Marine Reserve, California from co-authors Kiang and Parenteau (Kiang et al. 2022). The strain was maintained in liquid Marine-BG11 medium, MBG11, at 25°C under 15 μmol of photons $m^{-2}s-^{1}$ of continuous white fluorescent light (L36W-840, OSRAM).

For the experiment testing sensitivity to growth media and temperature, 50 mL inocula with initial optical density at 750 nm, OD_{750}, of 0.2 were grown either in MBG11 medium or in ASNIII medium, a common medium for marine cyanobacteria. MBG11, rich in iron, is the medium suggested for *A. marina*, but the presence of small agglomerates hinders the maintenance of fully axenic cultures. ASNIII, on the other hand, is a common medium for marine strains and facilitates the maintenance of clean cultures but has a lower salinity and a lower iron content. For a more detailed composition of the two media Table S1 can be consulted. Concurrently three different growth temperatures were tested: 20°C, 25°C, and 30°C.

Cultures were exposed to these six different conditions–20°C, 25°C, 30°C in either MBG11 or ASNIII—under continuous irradiation of 15 μmol of photons $m^{-2}s^{-1}$ of white light (TRUE-LIGHT 18T8, Lightfull). For each tested medium, four biological replicates were grown at 20°C, at 25°C, or at 30°C.

For the experiment testing sensitivity to light intensities, cultures with initial OD_{750} of 0.2 were grown at 25°C in liquid MBG11 in a multi-cultivator (Multi-Cultivator MC 1000-OD, Photon Systems Instruments, Czech Republic). Three biological replicates were exposed to 10, 20, 40, 60, 80, 100, and 150 μmol of photons $m^{-2}s^{-1}$ of continuous cold white light provided by built-in LEDs in the multi-cultivator.

Cultivation conditions for planetary simulations

Planetary conditions in terms of irradiance and atmosphere were simulated with a custom-made system extensively described in Battistuzzi et al. (2020, 2023a) and Claudi et al. (2021). Briefly, the set-up is comprised of three light sources and three growth chambers.

The light source for planetary simulation is a custom-made *starlight simulator*, SLS, which for this work was used to reproduce the irradiation of a quiescent (no or negligible UV) M dwarf (M7) in the range 350–850 nm (Fig. S1). For comparison, cultures were exposed also to a simulated solar light (SOL) and monochromatic FR light (FR). SOL light was provided by a custom-made visible-infrared light simulator with four independently manageable led channels in the range 365–800 nm. Channel 1 controls LEDs at 365 nm, 385 nm, 405 nm, 425 nm, and 500 nm; channel 2 controls SUNLIKE 5000 K and 690 nm LEDs; channel 3 (FR) controls LEDs at 730 and channel 4 (IR) controls LEDs at 750 nm and 780 nm. Channel intensity was regulated in order to accurately reproduce the Sun emission spectrum (Fig. S1). FR light peaked at 730 nm was provided with the illuminator described in Battistuzzi et al. (2023a) (Fig. S1a). For all light conditions, M7, SOL, FR, the total light intensity was 20 μmol of photons $m^{-2}s^{-1}$, resulting respectively in 7.38, 16.92, and 1.47 μmol of photons $m^{-2}s^{-1}$ of VIS light and 12.62, 3.08, and 18.53 μmol of photons $m^{-2}s^{-1}$ of FR light. A more detailed repartition of light in the different wavebands is available in Fig. S1c.

For experiments investigating acclimation to the M7 starlight, 50 mL of fresh cultures at OD_{750} 0.2 were transferred from white light to M7, SOL, and FR light. Growth and *in vivo* absorption were monitored periodically for 21 days, after which cultures were examined for physiological changes via *in vivo* absorption and fluorescence, pigment composition analysis and confocal microscopy.

For planetary simulations, where an anoxic primeval atmosphere was combined with stellar irradiation, *atmosphere simulating chambers*, ASCs, were used. Our ASCs are growth chambers that allow cultivation of organisms underneath both chosen light spectral irradiances—in this study M7, SOL and FR (Fig. S1b)—as well as prescribed gas composition. Inside the ASCs are one sensor for O_2 concentration (LOX-O2-S, SST sensing) and two sensors for CO_2 concentration (CO2M-20 and CO2M-100, SST sensing), which enable to monitor in real time and register the gas consumption and release during the experiment. In this work, the initial atmosphere inside the ASCs was composed of 95% nitrogen, N_2, and 5% CO_2, simulating an anoxic primeval planetary atmosphere. This composition approximates that of the Archean at ∼2.46 Ga just before the Great Oxidation Event (GOE), when atmospheric O_2 was negligible, CO_2 was 0.05–0.15 bar, and CH_4 had reduced to low levels >20 ppm (Catling and Zahnle 2020). We neglect the low CH_4 content for simplicity and note that it would not have affected the surface irradiance at this low ratio of CH_4 to the CO_2 (Trainer et al. 2006, Arney et al. 2016). The ASCs were then sealed over the course of experiments in order to monitor the impact of cyanobacteria on the initial atmosphere.

Raw data of gas concentrations in ppm registered during the experiments were converted in amount of μmol through Matlab R2018b (MathWorks) by applying the law of ideal gasses and considering the ASCs volume, 0.45 L (Battistuzzi et al. 2023a). Experiments with ASCs were run in parallel under M7, SOL and FR for four biological replicates.

Growth assessment

Growth of *A. marina* sp. str. Moss Beach was assessed through evaluation of optical density at 750 nm, OD_{750}, measured with a spectrophotometer (Cary100 UV-VIS, Agilent) against a blank (culture medium). OD_{750} was measured in intervals of 2–3 days. Maximum growth rate μ was calculated on the steepest slope of growth curves as follows:

$$\mu = \frac{\ln OD_{750f} - \ln OD_{750i}}{d} \quad (1)$$

were OD_{750f} is the OD_{750} value at the end of the interval, OD_{750i} is the value at the beginning of the interval and d is the number of days passed between the two points.

In vivo absorption, reflectance, and fluorescence

To record *in vivo* absorption spectra of cells, samples were centrifuged at 1400 *g* for 10 min at room temperature and the pellet was homogenized with a pestle. Six hundred microliter of fresh medium was added to solubilize the pellet and samples were analyzed with a Cary100 UV-VIS spectrophotometer (Agilent) inside quartz cuvettes. The opaque side of the cuvette was exposed to the light ray to correct the scattering (Shibata 1959, Amesz et al. 1961, Gan et al. 2014).

In vivo reflectance of cells was recorded with the set-up described in Liistro et al. 2026a). Briefly, a halogen lamp (Halostar Starlite 12 V 20 W G4, Osram) was used to irradiate 5 ml of liquid cultures with OD_{750} of 5 in a petri dish and reflectance was collected in the range 400–1000 nm with an optical fiber connected to a spectrometer (Flame, OceanOptics) via the SpectraSuite software (OceanOptics). Acquired spectra were normalized against a white reference. To compare *A. marina* sp. str. Moss Beach acclimated to the M7 simulated starlight, we analyzed cultures of *Synechocystis* sp. PCC6803 and *Chlorogleopsis fritschii* PCC6912 acclimated to the same simulated stellar spectra for control reflectance spectra. Information on the acclimation that these two strains perform under this condition can be found in Battistuzzi et al. (2023a, 2023c).

Low temperature (77 K) *in vivo* fluorescence emission spectra were recorded with a Cary Eclipse Fluorescence Spectrometer (Agilent). Two milliliter of culture were centrifuged at 1500 *g* for 10 min at 4°C and the pellet resuspended in 1 mL of glycerol 60% (w/v) and 10 mM Hepes pH 7.5. Samples were frozen in liquid nitrogen and kept in dark at −80°C until analysis. For the analysis, samples were excited at 440 nm and emission spectra were recorded between 600 nm and 900 nm. Low temperature (77 K, −196.15°C) during recording of emission spectra was maintained with liquid nitrogen.

Pigment content

For the extraction of lipophilic pigments, samples were centrifuged for 10 min at 17 500 *g* at 4°C and to the pellet were added an equal volume of 150–212 μm acid washed glass beads (SIGMA) and 50 μl of HPLC grade methanol 100%. Three cycles of cell rupture were executed with a Bullet Blender Storm Pro Homogenizer (Next Advance) for 15 s at maximum speed alternated with 30 s in ice. One hundred fifty microliter of methanol were added to the lysate and a last cycle of rupture was executed. Samples were centrifuged at 20 000 *g* for 10 min at 4°C and the supernatant, containing extracted pigments, was transferred to a new tube and kept in ice. 200 μl of methanol were added to the pellet and, after vortexing for resuspension, another centrifugation was performed. The supernatant was pooled with the previously obtained extract. These last steps were repeated until the supernatant appeared transparent, indicating full extraction of pigments. Samples were kept in dark at −20°C until analysis. Pigment extracts were analyzed with a Cary100 UV-VIS spectrophotometer (Agilent). Concentration of chlorophyll *a* and chlorophyll *d* were obtained with the following equations (Ritchie 2006):

$$Chl\ a\ \left(\frac{\mu g}{mL}\right) = Abs_{665} \bullet 13.0161 - Abs_{696} \bullet 3.1022 \quad (2)$$

$$Chl\ d\ \left(\frac{\mu g}{mL}\right) = Abs_{696} \bullet 12.9367 - Abs_{665} \bullet 0.3270 \quad (3)$$

To evaluate the relative content of chlorophyll and carotenoids, RP-HPLC analyses were conducted on pigment extracts. Analyses were performed with an Agilent 1100 series LC with a Lichrospher 100 RP column (250 mm length, 4 mm diameter) containing 5 μm silica particles coated by C-18 atom chains (Merck) as the stationary phase. The mobile phase consisted in buffer A (methanol: acetonitrile: water in ratio 42:33:25) and buffer B (methanol: acetonitrile: ethyl acetate in ratio 50:20:30). Buffer A and B were eluted in the column according to the protocol optimized by Gan and collaborators (Gan et al. 2014). The relative content was assessed by integrating the area of each peak in chromatograms at 440 nm for four biological replicates.

Confocal imaging

A. marina sp. str. Moss Beach cells were imaged with a confocal microscope (STELLARIS 8, Leica) to check for eventual changes in dimension, morphology and chlorophyll localization. Cells were excited by a laser diode with emission at 405 nm and imaged with two different channels to separate the fluorescence signal from chlorophyll *a* (672–689 nm) and chlorophyll *d* (705–739 nm).

Statistical analyses

Statistical analyses, ANOVA analysis (one-way or two-way ANOVA depending on the dataset) and Tukey's or Šídák's multiple comparison tests, were performed with the software GraphPad Prism v10.1.0 (GraphPad).

Results

Responses to nutrients, temperatures and light intensities in *A. marina* sp. str. Moss Beach

Acaryochloris marina sp. str. Moss Beach has not previously been characterized for the sensitivity of its growth to environmental parameters. Prior to the planetary simulation, we performed preliminary experiments investigating how temperature, growth media and light intensities affected the growth rate of this strain. Being originally developed for experiments on cyanobacteria, the simulator currently has the lower limit of operational temperature set at 25°C, which is slightly higher than the environmental temperature at which *A. marina* sp. str. Moss Beach was isolated, which was around 19°C. To understand whether this difference could have a non-negligible impact on the growth and performances of cells during the simulation, we followed their growth at three different temperatures: 20°C, reproducing the natural environment, 25°C, the target temperature, and 30°C, the temperature at which many cyanobacteria strains are maintained and at which we performed planetary simulations on other strains in the past (Battistuzzi et al. 2023a, 2023c), Liistro et al. 2024).

Concurrently, we evaluated the growth in two different saline media, Marine BG11 (MBG11) and artificial seawater (ASNIII) in combination with the three tested temperatures (Fig. 1). Based on the maximum growth rate registered during the experiment, the only temperature that significantly affected cell growth was 30°C,

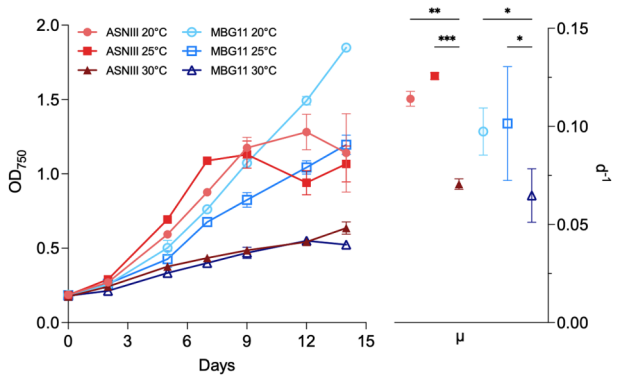

Figure 1 Growth of *Acaryochloris marina* sp. str. Moss Beach in different media and at different temperatures, in terms of values of OD_{750} and of growth rate (μ, d^{-1}). Cells were grown in Marine BG11 (MBG11, blue shades) and in artificial seawater (ASNIII, red shades). For each medium, three temperatures were tested: 20°C (round), 25°C (square), and 30°C (triangle). OD_{750} was registered every 2–3 days (left), and, from OD_{750} values, the maximum growth rate (μ) for each condition was calculated (right). Data are presented as the mean of four biological replicates, for values of μ one-way ANOVA was employed, ***: *P*-val <.0005, **: *P*-val <.005, *: *P*-val <.05. ASNIII: artificial seawater medium; MBG11: Marine BG11 medium.

in both MBG11 and ASNIII. Even though final values of OD_{750} were higher in cells grown at 20°C than at 25°C, growth rates registered in the exponential phase did not differ significantly. With regard to the media, ASNIII supported a faster initial growth, although maximum growth rates at the same temperature were not significantly different from rates in MBG11. Nonetheless, after 7 days for cells at 25°C, and 12 days for cells at 20°C, a cessation in the growth was encountered, suggesting that scarcity of essential nutrients in the ASNIII medium was reached in a shorter time than in MBG11, where OD_{750} kept gradually increasing.

To assess whether the composition and organization of the photosynthetic apparatus was affected by the tested condition, the diagnostic trait of Chl *a* and *d* content was analyzed. No significant differences were registered in any of the conditions in terms of μg of pigment per OD_{750} (Fig. 2), indicating cells maintain stable content of both Chl *a* and *d*. A slight difference occurred in cells grown at 30°C, which showed a higher percentage of Chl *d* both in ASNIII (98.23%) and in MBG11 (97.15%) than what registered in cells grown at 20°C and 25°C (around 94.50%).

Given the results of this preliminary screening, for further experiments cells were maintained in MBG11, which provides the appropriate amount of nutrients, at our target temperature of 25°C, since neither the growth nor the photosynthetic apparatus seem to be significantly affected.

With these parameters, experiments to identify the optimal light intensity for the acclimation to the M7 starlight were carried out. Indeed, prior to the simulation of planetary conditions, a step of acclimation to the stellar spectrum is needed, to understand whether a light with different spectral qualities triggers any change in the photosynthetic apparatus ascribable to any acclimation strategy. Acclimations may require time—days or weeks—to be implemented and detectable, and an evaluation of the optimal light intensity for the acclimation period is needed. In this case, the aim was to find a non-saturating light intensity to allow the identification of differences in growth capabilities and/or acclimation mechanisms when organisms are exposed to planetary simulations. Adding factors like a different spectrum and the anoxic atmosphere could make a saturating light become a stress factor and cells could incur photoinhibition.

To assess the most suitable light intensity, cultures at a starting OD_{750} of 0.2 were grown in a wide range of intensities, namely 10, 20, 40, 60, 80, 100, and 150 μmol of photons $m^{-2}s^{-1}$, maintaining the temperature at 25°C. Growth was followed by monitoring OD_{750}, from which the maximum growth rate μ was calculated (Fig. 3). The growth rate increased with increasing light intensities, up to 60 μmol of photons $m^{-2}s^{-1}$, where final OD_{750} reached the highest value of all conditions. With higher intensities, namely 80, 100, and 150 μmol of photons $m^{-2}s^{-1}$, growth was instead reduced, reaching low final OD_{750} values even though the maximum growth rates, registered in the first 2 days, was not significantly different from those exhibited at 10 and 20 μmol of photons $m^{-2}s^{-1}$. This growth rate was however not sustained over time in cells exposed to 80, 100, and 150 μmol of photons $m^{-2}s^{-1}$.

As for the previous experiment, diagnostic evaluation of the photosynthetic apparatus and pigment content was carried out on cells grown at the tested light intensities. *In vivo* absorption and low temperature fluorescence suggested no intensity had a major impact on cells—no marked differences were registered for any of the conditions (Fig. 4a, b). The highest mean values of Chl *a* and *d* content were registered at 10 and 20 μmol of photons $m^{-2}s^{-1}$, a progressive decline of mean chlorophyll concentrations was observed at stronger intensities, starting from 40 μmol of photons $m^{-2}s^{-1}$ and becoming statistically significant at 80, 100, and 150 μmol of photons $m^{-2}s^{-1}$. Nonetheless, the percentage of Chl *d* of the total chlorophyll content remained stable, around 94%, under all light intensities, except for cells exposed to 150 μmol photons $m^{-2}s^{-1}$, which showed a significant decrease (91.66%) (Fig. 4c). Relative carotenoid content was evaluated by integrating the area of peaks in HPLC chromatograms (Figs 4d and S2). In cells exposed to 10, 20, 40, and 60 μmol of photons $m^{-2}s^{-1}$ the percentage of carotenoids on the total pigment extract was in the range 27%–35%, while in cultures exposed to 80, 100, and 150 μmol of photons $m^{-2}s^{-1}$, the carotenoid percentage increased up to, respectively, 57.40%, 62.59%, and 76.02%.

Even though 40 and 60 μmol of photons $m^{-2}s^{-1}$ produce the highest growth rates, these intensities are nearly saturating as shown by the initial decline of mean chlorophyll content, which is exacerbated with increasing intensities. Further experiments were hence performed at 20 μmol of photons $m^{-2}s^{-1}$.

Planetary simulation: M dwarf starlight and primeval atmosphere

Different spectral qualities of light can trigger, in cyanobacteria, acclimations involving a remodeling of the photosynthetic apparatus (Sanfilippo et al. 2019). In order to assess whether this was the case for *A. marina* sp. str. Moss Beach under the simulated M dwarf spectrum, cells were transferred from white light to the simulated M dwarf starlight (M7), and, for comparison, to a simulated Solar starlight (SOL) and to monochromatic FR light (FR). Growth was followed for 21 days, a timing that canonically allows for light acclimations to be completely achieved (Ho et al. 2017, Liistro et al. 2026b). An initial lag phase of 6 days in growth was registered

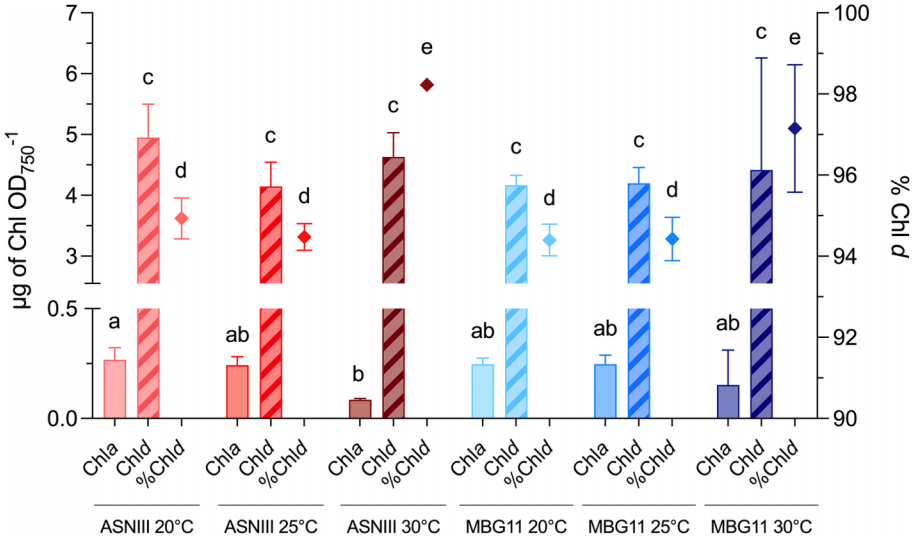

Figure 2 Pigment composition in *Acaryochloris marina* sp. str. Moss Beach grown in different media, ASNIII (red shades) and MBG11 (blue shades) and at different temperatures, 20°C (lighter shades), 25°C (normal shades), 30°C (darker shades). Chlorophyll *a* and *d* content are expressed as µg of pigment per OD_{750}, percentage of chlorophyll *d* on total chlorophyll content (rhombus); statistical significance was assessed with one-way ANOVA on at least three biological replicates. ASNIII: artificial seawater medium; MBG11: Marine BG11 medium; Chl *a*: chlorophyll *a*; Chl *d*: chlorophyll *d*.

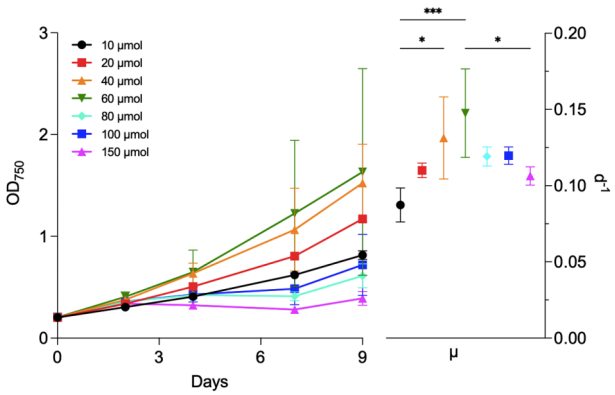

Figure 3 Growth of *Acaryochloris marina* sp. str. Moss Beach at different light intensities, in terms of values of OD_{750}, and of growth rate (µ, d^{-1}). Cells were grown at 10 (black, round), 20 (red, square), 40 (orange, triangle), 60 (green, inverted triangle), 80 (cyan, rhombus), 100 (blue, square), and 150 (pink, triangle) µmol of photons $m^{-2}s^{-1}$. OD_{750} was registered every 2–3 days (left), and, from OD_{750} values, the maximum growth rate (µ) for each condition was calculated (right). Data are presented as the mean of at least four biological replicates, for values of µ one-way ANOVA was carried out, ∗∗∗: *P*-val <.0005, ∗: *P*-val <.05.

in all light conditions, after which cells started to grow. Values of OD_{750} revealed a noticeable growth in both FR and M7 light, with a maximum rate respectively of 0.19 d^{-1} and 0.18 d^{-1}. On the other hand, cells exposed to SOL light had a lower final OD_{750} as well as a lower maximum growth rate (0.15 d^{-1}) (Fig. 5).

During acclimation to the different spectra, *in vivo* absorbance of cells was registered periodically, with no significant change of absorption spectra: after 21 days, there was no alteration from cell absorption spectrum at day zero, in any of the conditions (Fig. 6a). Comparably, chlorophyll content as well as the percentage of Chl *d* on the total chlorophyll content remained stable in all the tested conditions (Fig. 6b). Low temperature fluorescence coherently indicated that no modification involving the emission ranges of the photosynthetic apparatus were activated under M dwarf light, nor in any of the other light regimes: emission spectra were analogous, with the main peak being at 748 nm in all of the conditions (Fig. 6c). Finally, cells were imaged with confocal microscopy to evaluate eventual changes in morphology or in the localization of chlorophylls (Fig. 6d). Micrographs revealed similar shape and dimension of cells acclimated to all tested light, as well as comparable spatial distribution of Chl *a* and *d* autofluorescence.

A. marina sp. str. Moss Beach cultures acclimated to SOL, FR, and M7 light were used to evaluate the response and performances in simulated planetary conditions comprehensive of a modified atmosphere. Liquid cultures of OD_{750} 0.55 were placed in the atmosphere-simulating chambers, ASCs, supplied with an initial anoxic atmosphere, under the respective light source (SOL, FR, and M7) for 72 hours.

After 72 h of exposure, strong growth was registered in all conditions (Fig. 7a), indicating that the initial anoxic atmosphere was not preventing cell survival and reproduction. Interestingly, M7 light promoted the strongest growth, with cells in SOL and FR having a lower final OD_{750}.

Cells in M7 showed a higher CO_2 consumption and O_2 release, with final values of ΔCO_2 and ΔO_2 being respectively the lowest and the highest registered with respect to SOL and FR (Fig. 7b, c). As highlighted in Fig. 7d, e, under M7 and FR light the production rates of

O_2 and CO_2 respectively increase and decrease faster than in SOL light, where indeed the lowest final mean OD_{750} value was encountered.

To assess the surface biosignature that an organism with the features of *A. marina* sp. str. Moss Beach could generate, the reflectance spectrum of cells was recorded, presented in Fig. 8 along with the reflectance spectra of two other cyanobacterial strains previously tested under the starlight simulator, *Synechocystis* sp. PCC6803 and *Chlorogleopsis fritschii* PCC6912 (Battistuzzi et al. 2023a, 2023c). Reflectance spectra were recorded on cultures

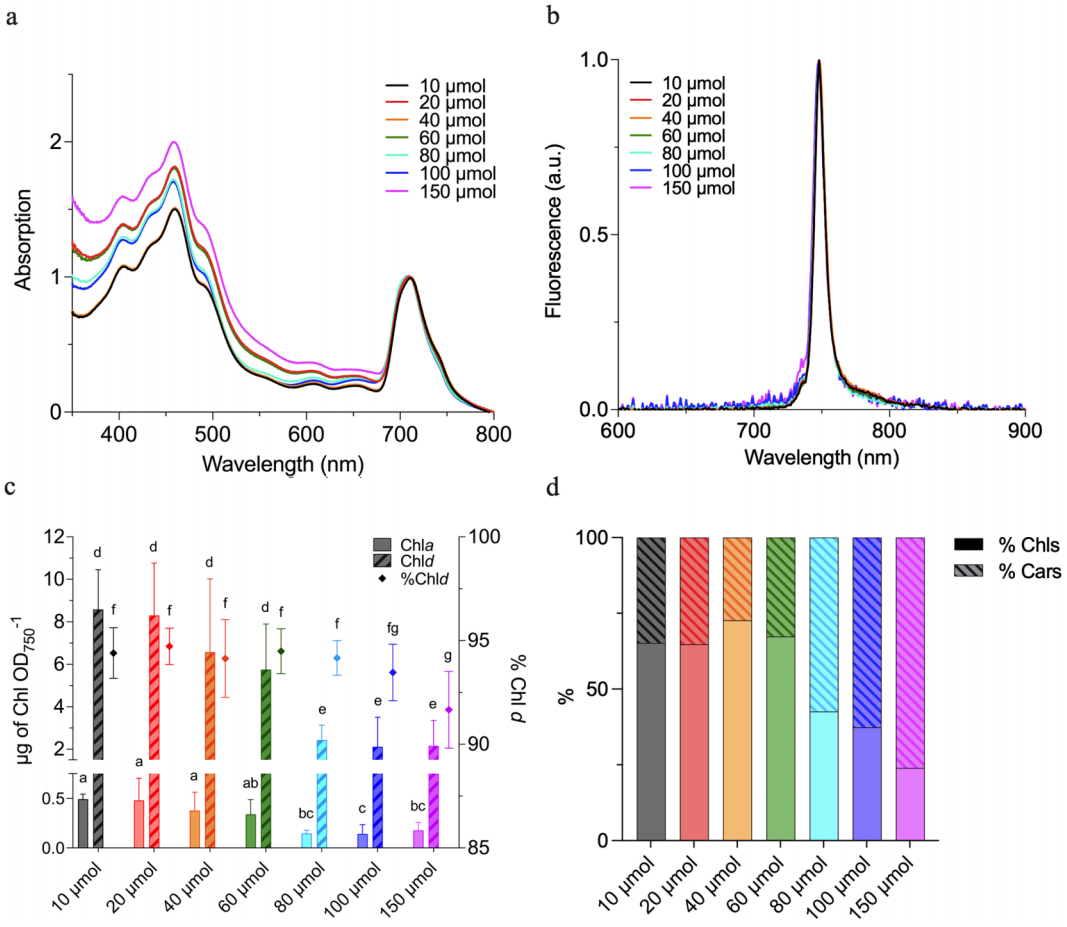

Figure 4 Pigment composition and photosynthetic apparatus organization in *Acaryochloris marina* sp. str. Moss Beach grown at different light intensities, 10 (black), 20 (red), 40 (orange), 60 (green), 80 (cyan), 100 (blue), and 150 (pink) µmol of photons $m^{-2}s^{-1}$. (a) *in vivo* absorbance spectra of cells normalized at 710 nm, (b) low temperature (77 K) fluorescence emission spectra of cells, normalized at the maximum peak (748 nm), (c) chlorophyll *a* (full pattern) and *d* (stripe pattern) content expressed as µg of pigment per OD_{750} and chlorophyll *d* percentage on total chlorophyll content (rhombus); statistical significance was checked with one-way ANOVA on at least four biological replicates, (d) percentage of total chlorophylls (full pattern) and total carotenoids (stripe pattern) in cells extracts. Chl *a*: chlorophyll *a*; Chl *d*: chlorophyll *d*.

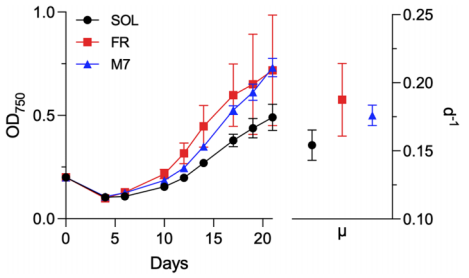

Figure 5 Growth of *A. marina* sp. str. Moss Beach during acclimation to the simulated stellar spectra. Growth of cells exposed to solar (SOL, black), far-red (FR, red) and M dwarf (M7, blue) light was monitored with measures of OD_{750} every 2–4 days (left), from these values, the maximum growth rate (µ) during the 21 days was measured (right). Data are presented as the mean of three biological replicates. SOL: simulated solar light; FR: far-red light; M7: simulated M dwarf starlight.

acclimated to M7 light, *in vivo* absorption of *S.* sp. PCC6803 and *C. fritschii* PCC6912 acclimated to SOL and M7 light are available in Fig. S3.

The reflectance spectrum of oxygenic phototrophs can be quite diverse in the 400–650 nm region, because pigment types and concentration can vary severely. This was perceivable in the spectra of *S.* sp. PCC6803, *C. fritschii* PCC6912, and *A. marina* sp. str. Moss Beach. A decrease of reflectance due to Chl *a* (at 440 nm and 680 nm) and phycocyanin (630 nm) absorption is found in *S.* sp. PCC6803 and *C. fritschii* PCC6912 with different intensities, ascribable to a different concentration of these pigments in the two species. On the other hand, this pattern is not found in *A. marina* sp. str. Moss Beach, that lacks phycocyanin and has minor content of Chl *a* with respect to the predominant Chl *d*, resulting in reflectance depressions at different wavelengths (460 nm and 700 nm). Despite differences in this region, reflectance of oxygenic phototrophs is typically characterized by a steep increase in reflectance between 680 nm and 750 nm, as noticeable from the spectrum of *S.* sp. PCC6803. This rise originates from the contrast of the high absorption capacity of Chl *a* in the red and the scattering of infrared light due to the change in the refractive index between cellular membranes and the medium. This pattern, called the Vegetation Red-Edge, VRE, is detectable in the reflectance spectra of Earth surface areas covered by oxygenic photosynthetic

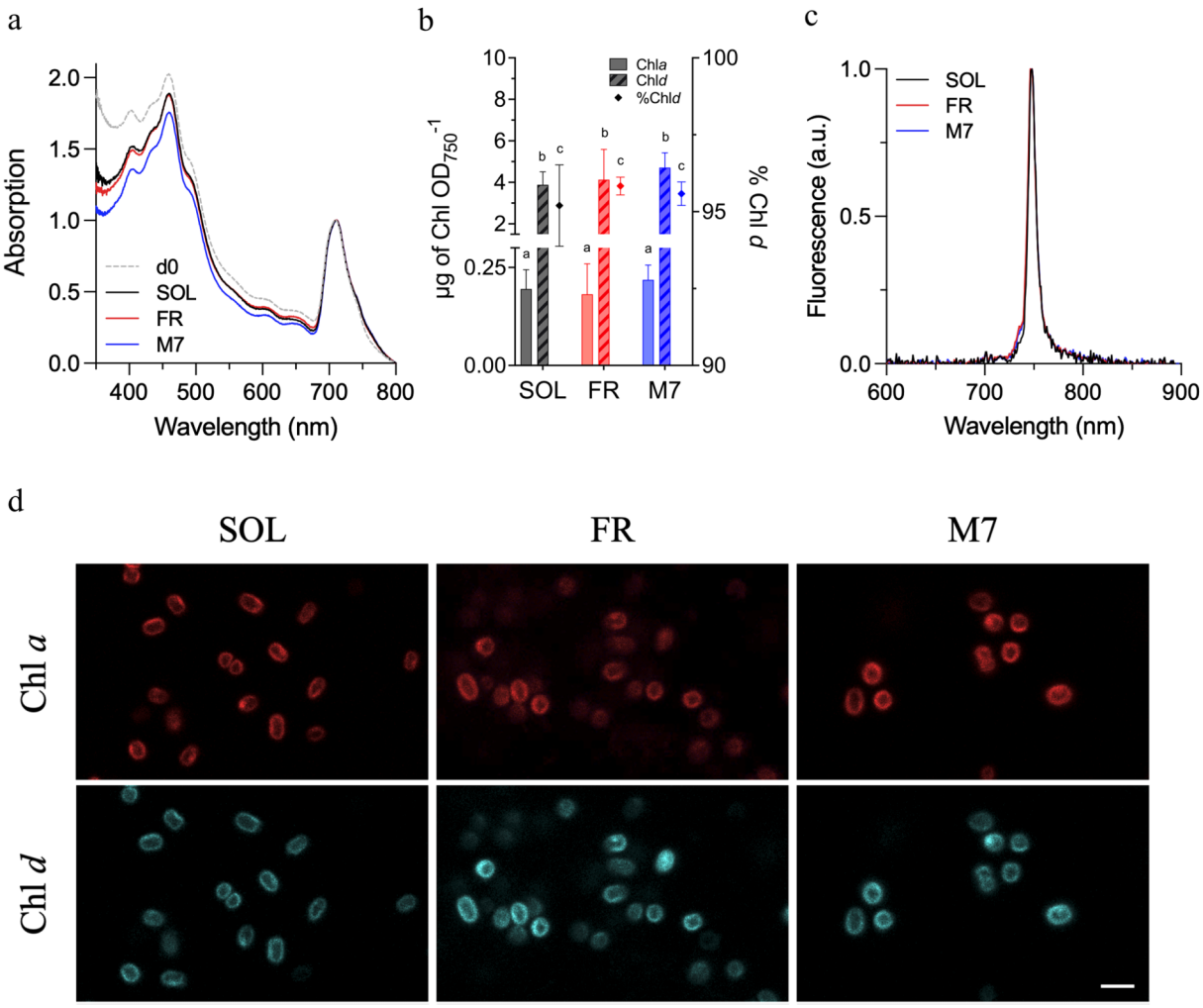

Figure 6 *A. marina* sp. str. Moss Beach features after acclimation to SOL, M7, FR light. (a) *in vivo* absorption spectra of cell before (day zero, d0) and after acclimation; (b) content of chlorophyll *a* (full pattern) and *d* (stripe pattern) in terms of µg of pigment per OD_{750}, percentage of chlorophyll *d* in cell extracts; statistical significance was assessed with one-way ANOVA on three biological replicates; (c) low temperature (77 K) fluorescence emission spectra of cells; (d) representative confocal images of respectively SOL-, FR- and M7-acclimated cells, red indicates the autofluorescence of chlorophyll *a*, cyan indicates the autofluorescence of chlorophyll *d*, scale bar corresponds to 2.5 µm. d0: day zero; SOL: simulated solar light; FR: far-red light; M7: simulated M dwarf starlight; Chl *a*: chlorophyll *a*; Chl *d*: chlorophyll *d*.

organisms. This feature resulted altered in *C. fritschii* PCC6912 cells acclimated to M7 light, where a shift in reflectance was present above 700 nm, likely ascribable to the presence of small amounts of chlorophyll *d* and *f*. *In vivo* absorption of cultures used to obtain the reflectance spectra highlight indeed a shoulder of absorption beyond 700 nm in *C. fritschii* PCC6912, indicating the occurrence of the FaRLiP response in this strain under M7 irradiation (Fig. S3, Battistuzzi et al. 2023a). In *A. marina* sp. str. Moss Beach, due to the abundance of Chl *d*, the steep rise in reflectance was instead completely shifted toward longer wavelengths, between 710 nm and 780 nm, in what could be referred to as a *Chl* d-*near-infra-red edge,* or Chl *d*-NIR edge.

Discussion

Some of the planned space missions from NASA and ESA are aimed at characterizing the atmospheres of exoplanets, also in the search for biosignatures. In particular, HWO (NASA) will be able to detect the presence of O_2, that astrobiologists indicate as one of the strongest biosignatures to search for. As on Earth the accumulation of O_2 in the atmosphere is due to oxygenic photosynthesis, operated by cyanobacteria, algae and plants, for years the community has been debating on the feasibility and efficiency of this metabolism on exoplanets. In this work we focused on this possibility to occur around M dwarf stars, as they are considered good targets for their long lifespan and the abundancy of rocky exoplanets identified as habitable harbored in their stellar systems (Gale and Wandel 2016, Shields et al. 2016). The challenge for oxygenic photosynthesis to have evolved with an M dwarf spectrum resides in the long wavelength limit of this metabolism. On Earth, oxygenic photosynthetic organisms rely on visible light, and can only marginally harvest FR light, while M dwarfs emission spectra offer very low visible and high FR and IR irradiance (Chabrier et al. 1996).

Laboratory simulations have however demonstrated how an M dwarf spectrum can support strong growth in cyanobacteria and microalgae, and moderate growth in non-vascular

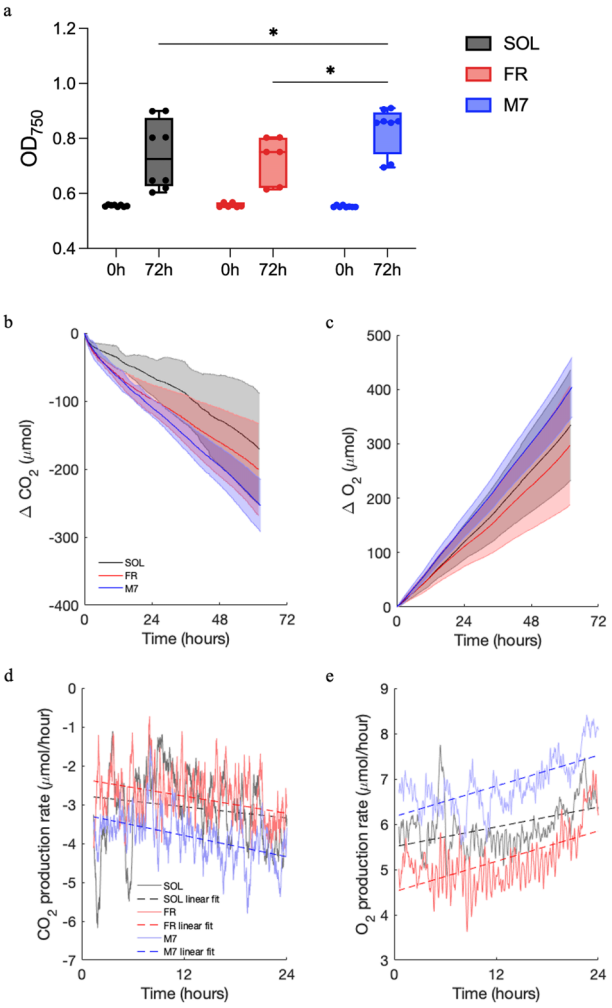

Figure 7 Growth and gas consumption of *Acaryochloris marina* sp. str. Moss Beach inside the ASCs under SOL, FR, and M7 light. (a) initial (0 h) and final (72 h) OD_{750} values, (b) variation of CO_2 concentration, (c) variation of O_2 concentration, (d) CO_2 production rate, (e) O_2 production rate (negative values indicate consumption). (a) shows individual values (dots) and average values (horizontal line inside the box plot), ∗: *P*-val: ≤.05. For (b) and (c) T_0 was set at 5 h to exclude the initial period of gas equilibration inside the ASCs. For (d) and (e) the last 24 h of exposure were considered, to exclude the initial acclimation of organisms to the anoxic/microoxic environment. SOL: simulated solar light; FR: far-red light; M7: simulated M dwarf starlight; CO_2: carbon dioxide; O_2: oxygen.

plants that evolved to harvest visible light ((Battistuzzi et al. 2023a, 2023b, 2023c, Liistro et al. 2024, Boccia et al. 2026). Nonetheless, this does not imply that analogous organisms should be expected to have evolved under such spectrum: a red-shifted irradiance might have selected "red-shifted adaptations" as for instance modified antennae (Chitnavis et al. 2024) or *two color* reaction centers absorbing respectively visible and near-infra-red light. (Takizawa et al. 2017).

Considering the red-shifted adaptations of oxygenic photosynthesis that have evolved on Earth, in this work we tested the Moss Beach strain of *Acaryochloris marina*, a unique species with Chl *d*-bearing reaction centers and permanent red-shifted absorption, to assess whether its photosynthetic apparatus is a good fit under

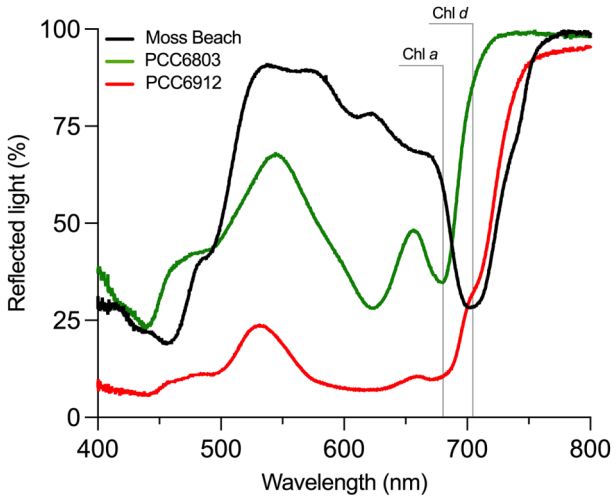

Figure 8 *In vivo* reflectance spectra of liquid cultures of *A. marina* sp. str. Moss Beach (black), *Synechocystis* sp. PCC6803 (green) and *Chlorogleopsis fritschii* PCC6912 (red) acclimated to the M7 light recorded with a Flame spectrometer (OceanOptics). Moss Beach: *A. marina* sp. str. Moss Beach; 6803: *Synechococcus* sp. PCC6803; 6912: *Chlorogleopsis fritschii* PCC6912; Chl *a*: chlorophyll *a*; Chl *d*: chlorophyll *d*.

M dwarf-like irradiance, evaluating both time courses of OD_{750} and O_2 production rates.

Chl *d* spectral type

While Kiang et al. (2022) observed *A. marina* sp. str. Moss Beach to have a spectral peak at 705 nm, our culture from a sample directly obtained from their lab exhibited a spectral peak at 710 nm. Shifts in the spectral peak in the same *A. marina* strain has been observed also for other strains (Min Chen, personal communication), which is likely due to photoacclimation to different growth conditions, the mechanisms for which are still being elucidated. Due to the divergence of their light harvesting systems and chlorophyll environment, *A. marina* strains exhibit a high variation in the fluorescence properties of Chl *d* and in the spectral features. Ulrich and colleagues (2024) identified three main spectral types depending on fluorescence emission features, which reflect differences in Chl energy levels and in chl-binding proteins. From the *intermediate-wavelength* spectral type, with emission maximum at 727–731 nm, diverged both the *short-wavelength* and the *long-wavelength* spectral types, with emission maxima respectively at 721–724 nm and 738–748 nm. Our analysis of low temperature fluorescence identified the spectral type of the strain Moss Beach, that, presenting a fluoresce peak at 748 nm, should be included in the *longer wavelength* group, to which also its close relative *A. marina* S15 belongs (Kiang et al. 2022, Ulrich et al. 2024). This locates *A. marina* sp. str. Moss Beach in the group of oxygenic photosynthetic organisms with the strongest red-shifted constitutive emission among the types differentiated by Ulrich et al. (2024), making it an excellent target to test Earth "red-shifted adaptions" in M dwarf simulated light. Very recently, an even further red-shifted strain was discovered, with the emission maximum at ∼760 nm (Oliver et al. 2026).

Absence of chromatic acclimation

Results of the preliminary acclimation to the simulated stellar spectra, M7, reproducing an M dwarf star, highlight how, differently from other species previously tested, *A. marina* sp. str. Moss Beach does not need to modulate the pigment content nor its photosynthetic apparatus in order to efficiently grow with the M7 light. When tested in the same set up, cyanobacteria like *Chlorogleopsis fritschii* sp. PCC6912 and *Synechococcus* sp. PCC7335, underwent severe remodeling of the photosynthetic apparatus, acclimating to harvest the abundant red and FR light available. *C. fritschii* PCC6912 exhibited the FaRLiP response (Battistuzzi et al. 2023a), maximizing FR light absorption, while *S.* PCC7335 strongly modulated the content of accessory pigments via chromatic acclimation type 3, maximizing red light absorption (Liistro et al. 2024). The unaltered absorption features and pigment content observed for *A. marina* sp. str. Moss Beach underlined, instead, how this strain is already well suited to photosynthesize under the simulated M7 stellar spectrum, growing even better than when exposed to the simulated solar light, SOL.

Growth rate and O_2 evolution under M dwarf simulated light

Interestingly, during acclimation, growth rates were higher than that exhibited in previous experiments conducted in white light: SOL, FR, and M7 lights all provide a portion of FR photons, in different amounts, which appears to be crucial for this strain to drive faster growth. Indeed, at the end of the acclimation experiment performed in terrestrial atmosphere, the highest OD_{750} were observed in M7 light and monochromatic FR light, while in SOL light, which provided the lowest flux of FR photons of all three tested lights, the final mean OD_{750} was the lowest. Studies conducted on *A. marina* sp. str. MBIC11017, found similar results: for this strain as well, a stronger growth was registered when cells were exposed to FR light rather than visible light. This was paired with a stronger photosynthetic rates, indicating longer wavelength drive photosynthesis more efficiently than visible ones (Behrendt et al. 2012).

Considering all the conditions tested in this study, *A. marina* sp. str. Moss Beach showed a maximal growth rate reaching 0.19 d^{-1}, comparable to that registered in the reference strain of *A. marina*, MBIC11017 (Swingley et al. 2005).

With *A. marina* sp. str. Moss Beach acclimated to SOL, FR and M7 spectra, we then proceeded with planetary simulation, combining the light treatment with a simulated planetary primeval atmosphere non-oxygenated (95% N_2 and 5% CO_2). Cells grew consistently in all the light conditions, suggesting the initial absence of oxygen had no major detrimental effects. As early oxygenic cyanobacteria in the Archean would have had to function in largely anoxic atmospheric conditions (Lyons et al. 2014); therefore, our experiment demonstrates the viability of growth at low O_2. Most importantly, in the anoxic atmosphere, the M7 starlight promoted the highest growth with respect with SOL and FR light. Cells were indeed efficiently sequestrating CO_2 and producing O_2, having the strongest rates under the simulated starlight when compared with cells in SOL and FR light.

All the cyanobacteria species examined in our planetary experiments efficiently sequestered CO_2 and produced O_2, however, the grater O_2 productivity in *A. marina* sp. str. Moss Beach is noticeable if compared with the strains previously tested in this combination of stellar light and atmosphere simulation. After 72 h of exposure to simulated planetary conditions (starlight spectrum coupled with primeval atmosphere), we registered the production of ∼400 μmol of O_2 in *A. marina* sp. str. Moss Beach. *C. fritschii* PCC6912 and *S.* sp. PCC6803 reached similar O_2 production after 48 h under the same spectrum and in the same atmosphere tested in this work (Battistuzzi et al. 2023c), which is interesting considering they are both fast-growing strains and they were exposed to a higher total irradiance (30 μmol of photons $m^{-2}s^{-1}$). *S.* sp. PCC7335, a relatively slow-growing organism, took 7 days to produce the same amount under the same spectrum—however, it must be considered that the total irradiance of the experiment was set to 10 μmol of photons $m^{-2}s^{-1}$, half the one used in this study (Liistro et al. 2024).

Implication for exoplanet biosignature detection

If photosynthetic metabolisms like the one selected in *A. marina* sp. str. Moss Beach have evolved outside our Solar System, our data support the potential to generate atmospheric biosignature via the release of O_2. Of course, the planetary oxygenation time and the diversification and spread of oxygenic phototrophs would definitively control on the potential accumulation of this gas, hence on the possibility of its detection.

Moreover, the reflectance spectrum of *A. marina* sp. str. Moss Beach cells underlines how, if such metabolism is present on exoplanets orbiting M dwarf stars, and if it could be utilized in potentially far-red vegetation, its fingerprint would be highly characteristic, with a VRE profoundly shifted toward longer wavelength, becoming a *near-infra-red-edge*, NIRE.

Overall, *A. marina* sp. str. Moss Beach is an excellent example of how evolution on Earth has led oxygenic photosynthesis to red-shifted adaptations that can efficiently photosynthesize with an M dwarf like spectrum, underlining the possibility of natural selection to push highly functional metabolisms forward their energetic limits, as in the case of *A. marina* species.

Conclusions

The *A. marina* species constitute fine evidence of how evolutionary pressure can lead oxygenic photosynthesis not only toward visible-harvesting forms but also toward constitutive red-shifted forms.

In this work, the Moss Beach strain of *A. marina* was tested for the first time under a simulated M dwarf light, evaluating also its capacity to produce O_2 in an anoxic atmosphere enriched in CO_2.

The results of this work highlight how the photosynthetic apparatus of *A. marina* sp. str. Moss Beach represents a very good, constitutively red-shifted, fit for oxygenic photosynthesis under M dwarf stars, leading to the release of considerable amounts of O_2 with a strong impact on the initial anoxic atmosphere. Surprisingly the O_2 production rate of this Chl *d* cyanobacterium was comparable to that of Chl *a*-only cyanobacteria that have been previously studied. If evolved on exoplanets orbiting around an M dwarf, this kind of metabolism could hence generate a gaseous biosignature. The data of O_2 release here presented are of crucial interest for exoplanet habitability models and represent a reference to

interpret the data that will eventually result from future space missions like ARIEL (ESA) and HWO (NASA), that are going to investigate exoplanets' atmospheres. Regarding the possibility of such organisms to generate a surface biosignature, the pigment content of *A. marina* sp. str. Moss Beach is unaltered under the solar or the M dwarf spectra, resulting in a characteristic reflectance spectrum with a Vegetation Red-Edge sensibly shifted toward longer wavelengths, in a *NIR edge*.

The long wavelength limit for oxygenic photosynthesis remains an open question. Trade-offs in the efficiency and resilience of far-red phototrophy with lower energy photons have been identified in comparisons of enzyme turnover and electron transfers in Chl *a*, FaRLiP, and *A. marina* Chl *d* species (Viola et al. 2022), but even algae have been found tuned to FR light (Wolf and Blankenship 2019), and higher plants demonstrate oxygen evolution out to 750 nm or longer (Zhen 2020). The Chl *d*-NIR-edge we have observed in *A. marina* sp. str. Moss Beach is likely only one NIR edge along a continuum, which future work should continue to constrain relative to controls at the molecular and environmental scales.

Acknowledgments

Authors would like to thank Marianna Quadri, Mariano Battistuzzi, Lorenzo Cocola and the staff of the Imaging Facility of the Department of Biology of the University of Padova for the scientific and technical support.

Author contributions

Elisabetta Liistro (Conceptualization, Formal analysis, Investigation, Methodology, Data curation, Visualization, Writing—original draft, Writing—review and editing), Beatrice Boccia (Formal analysis, Data curation, Writing—review and editing), Mary Niki Parenteau (Resources, Conceptualization, Writing—review and editing), Nancy Y. Kiang (Resources, Conceptualization, Writing—review and editing), and Nicoletta La Rocca (Resources, Conceptualization, Investigation, Data Curation, Supervision, Writing—original draft, Writing—review and editing)

Supplementary material

Supplementary material is available at *FEMSMC Journal* online.

Conflicts of interest

None declared.

Funding

The research was funded by the Italian Space Agency through the "ASTERIA" project (ASI N. 2023-5-U.0) and by the Department of Biology of the University of Padova (Italy) via intramural grants.

References

Amesz J, Duysens LNM, Brandt DC. Methods for measuring and correcting the absorption spectrum of scattering suspensions. *J Theor Biol* 1961;**1**:59–74. https://doi.org/10.1016/0022-5193(61)90026-1

Anglada-Escudé G, Amado PJ, Barnes J *et al.* A terrestrial planet candidate in a temperate orbit around Proxima Centauri. *Nature* 2016;**536**:437–40. https://doi.org/10.1038/nature19106

Antonaru LA, Rad-Menéndez C, Mbedi S *et al.* Evolution of far-red light photoacclimation in cyanobacteria. *Curr Biol* 2025;**35**:2539–53. https://doi.org/10.1016/j.cub.2025.04.038

Arney G, Domagal-Goldman SD, Meadows VS *et al.* The Pale Orange Dot: the spectrum and habitability of Hazy Archean Earth. *Astrobiology* 2016;**16**:873–99. https://doi.org/10.1089/ast.2015.1422

Badshah SL, Mabkhot Y, Al-Showiman SS. Photosynthesis at the far-red region of the spectrum in *Acaryochloris marina*. *Biol Res* 2017;**50**:16. https://doi.org/10.1186/s40659-017-0120-0

Battistuzzi M, Cocola L, Claudi R *et al.* Oxygenic photosynthetic responses of cyanobacteria exposed under an M-dwarf starlight simulator: implications for exoplanet's habitability. *Front Plant Sci* 2023a;**14**:1070359. https://doi.org/10.3389/fpls.2023.1070359

Battistuzzi M, Cocola L, Liistro E *et al.* Growth and photosynthetic efficiency of microalgae and plants with different levels of complexity exposed to a simulated M-dwarf starlight. *Life* 2023b;**13**:1641. https://doi.org/10.3390/life13081641

Battistuzzi M, Morlino MS, Cocola L *et al.* Transcriptomic and photosynthetic analyses of Synechocystis sp. PCC6803 and *Chlorogloeopsis fritschii* sp. PCC6912 exposed to an M-dwarf spectrum under an anoxic atmosphere. *Front Plant Sci* 2023c;**14**:1322052. https://doi.org/10.3389/fpls.2023.1322052

Battistuzzi M, Cocola L, Salasnich B *et al.* A new remote sensing-based system for the monitoring and analysis of growth and gas exchange rates of photosynthetic microorganisms under simulated non-terrestrial conditions. *Front Plant Sci* 2020;**11**:182. https://doi.org/10.3389/fpls.2020.00182

Behrendt L, Schrameyer V, Qvortrup K *et al.* Biofilm growth and near-infrared radiation-driven photosynthesis of the chlorophyll d-containing cyanobacterium *Acaryochloris marina*. *Appl Environ Microb* 2012;**78**:3896–904. https://doi.org/10.1128/AEM.00397-12

Boccia B, Battistuzzi M, Liistro E *et al.* Growth of phylogenetically diverse microalgae under Far-Red light enriched spectra: implication for space missions' sustainability. *Front Microbiol* 2026;**17**:1833797. https://doi.org/10.3389/fmicb.2026.1833797

Catling DC, Zahnle KJ., The Archean atmosphere. *Sci Adv* 2020;**6**. https://doi.org/10.1126/sciadv.aax1420

Cavalazzi B, Westall F., Advances in astrobiology and biogeophysics. In *Biosignatures for Astrobiology*. Springer Nature Switzerland, 2019.

Chabrier G, Baraffe I, Plez B. Mass-luminosity relationship and lithium depletion for very low mass stars. *Astrophys J* 1996;**459**:L91–94. https://doi.org/10.1086/309951

Chan Y-W, Nenninger A, Clokie SJH. *et al.* Pigment composition and adaptation in free-living and symbiotic strains of *Acaryochloris marina*. *FEMS Microbiol Ecol* 2007;**61**:65–73. https://doi.org/10.1111/j.1574-6941.2007.00320.x

Chen M, Quinnell RG, Larkum AWD. Chlorophyll d as the major photopigment in Acaryochloris marina. *J Porphyrins Phthalocyanines* 2002;**06**:763–73. https://doi.org/10.1142/S1088424602000889

Chitnavis S, Gray C, Rousouli I *et al.* Optimizing photosynthetic light-harvesting under stars: simple and general antenna models. *Photosynth Res* 2024;**162**:75–92. https://doi.org/10.1007/s11120-024-01118-1

Claudi R, Alei E, Battistuzzi M *et al.* Super-earths, m dwarfs, and photosynthetic organisms: habitability in the lab. *Life* 2021;**11**:10. https://doi.org/10.3390/life11010010

Claudi R, Alei E. Biosignatures search in habitable planets. *Galaxies* 2019;**7**:82. https://doi.org/10.3390/galaxies7040082

Elias E, Oliver TJ, Croce R. Oxygenic photosynthesis in far-red light: strategies and mechanisms. *Annu Rev Phys Chem* 2024;**75**:231–56. https://doi.org/10.1146/annurev-physchem-090722-125847

Feinberg LD, Sitarski BN, McElwain MW *et al. Habitable Worlds Observatory's Concept and Technology Maturation: initial Feasibility and Trade Space Exploration*. (arXiv:2601.11803). arXiv, 2026, https://doi.org/10.48550/arXiv.2601.11803

Gale J, Wandel A. The potential of planets orbiting red dwarf stars to support oxygenic photosynthesis and complex life. *Int J Astrobiol* 2016;**16**:1–9. https://doi.org/10.1017/S1473550415000440

Gan F, Zhang S, Rockwell NC *et al.* Extensive remodeling of a cyanobacterial photosynthetic apparatus in far-red light. *Science* 2014;**345**:1312–7. https://doi.org/10.1126/science.1256963

Gausman HW, Gerbermann AH, Wiegand CL *et al.* Reflectance differences between crop residues and bare soils. *Soil Science Soc Amer J* 1975;**39**:752–5. https://doi.org/10.2136/sssaj1975.03615995003900040043x

Grant L. Diffuse and specular characteristics of leaf reflectance. *Remote Sens Environ* 1987;**22**:309–22. https://doi.org/10.1016/0034-4257(87)90064-2

Gray C, Chitnavis S, Buja T *et al.* Predicting the diversity of photosynthetic light-harvesting using thermodynamics and machine learning. *PLoS Comput Biol* 2025;**21**:e1012845. https://doi.org/10.1371/journal.pcbi.1012845

Ho MY, Gan F, Shen G. *et al.* Far-red light photoacclimation (FaRLiP) in Synechococcus sp. PCC 7335. II.Characterization of phycobiliproteins produced during acclimation to far-red light. *Photosynth Res* 2017;**131**:187–202. https://doi.org/10.1007/s11120-016-0303-5

Ho MY, Soulier NT, Canniffe DP *et al.* Light regulation of pigment and photosystem biosynthesis in cyanobacteria. *Curr Opin Plant Biol* 2017;**37**:24–33. https://doi.org/10.1016/j.pbi.2017.03.006

Hsu DC, Ford EB, Terrien R. Occurrence rates of planets orbiting M Stars: applying ABC to Kepler DR25, Gaia DR2, and 2MASS data. *Mon Not R Astron Soc* 2020;**498**:2249–62. https://doi.org/10.1093/mnras/staa2391

Kaltenegger L. How to characterize habitable worlds and signs of life. *Annu Rev Astron Astrophys* 2017;**55**:433–85. https://doi.org/10.1146/annurev-astro-082214-122238

Kasting JF, Whitmire DP, Reynolds RT. Habitable zones around main sequence stars. *Icarus* 1993;**101**:108–28. https://doi.org/10.1006/icar.1993.1010

Kiang NY, Segura A, Tinetti G *et al.* Spectral signatures of photosynthesis. II. Coevolution with other stars and the atmosphere on extrasolar worlds. *Astrobiology* 2007a;**7**:252–74. https://doi.org/10.1089/ast.2006.0108

Kiang NY, Siefert J,Govindjee *et al.* Spectral signatures of photosynthesis. I. Review of Earth organisms. *Astrobiology* 2007b;**7**:222–51. https://doi.org/10.1089/ast.2006.0105

Kiang NY, Swingley WD, Gautam D. *et al.* Discovery of Chlorophyll d: isolation and characterization of a far-red cyanobacterium from the original site of manning and strain (1943) at Moss Beach, California. *Microorganisms* 2022;**10**:819. https://doi.org/10.3390/microorganisms10040819

Kopparapu RK, Ramirez R, Kasting JF *et al.* Habitable zones around main-sequence stars: new estimates. *Astrophys J* 2013;**765**:131. https://doi.org/10.1088/0004-637X/765/2/131

Larkum AWD, Kühl M. Chlorophyll d: the puzzle resolved. *Trends Plant Sci* 2005;**10**:355–7. https://doi.org/10.1016/j.tplants.2005.06.005

Liistro E, Battistuzzi M, Cocola L *et al. Synechococcus* sp. PCC7335 responses to far-red enriched spectra and anoxic/microoxic atmospheres: potential for astrobiotechnological applications. *Plant Physiol Biochem* 2024;**213**:108793. https://doi.org/10.1016/j.plaphy.2024.108793

Liistro E, Battistuzzi M, Storti M *et al.* Thylakoids reorganization enables driving photosynthesis under far-red light in the microalga *Nannochloropsis gaditana*. *New Phytol* 2026a;**249**:1785–99. https://doi.org/10.1111/nph.70786

Liistro E, Calcinoni A, Agostini A *et al.* Enhanced carotenoid photoprotection in far-red light acclimated *Chroococcidiopsis thermalis*. *Plant Physiol Biochem* 2026b;**233**:111265. https://doi.org/10.1016/j.plaphy.2026.111265

Lyons TW, Reinhard CT, Planavsky NJ. The rise of oxygen in Earth's early ocean and atmosphere. *Nature* 2014;**506**:307–15. https://doi.org/10.1038/nature13068

Méndez A, Rivera-Valentín EG, Schulze-Makuch D. *et al.* Habitability models for astrobiology. *Astrobiology* 2021;**21**:1017–27. https://doi.org/10.1089/ast.2020.2342

Miyashita H, Ikemoto H, Kurano N *et al.* Chlorophyll d as a major pigment. *Nature* 1996;**383**:402. https://doi.org/10.1038/383402a0

Mohr R, Voß B, Schliep M. *et al.* A new chlorophyll d-containing cyanobacterium: evidence for niche adaptation in the genus Acaryochloris. *ISME J* 2010;**4**:1456–69. https://doi.org/10.1038/ismej.2010.67

Oliver TJ, Elias E, Consoli G. *et al.* Far-red chlorophyll d clusters extend photosystem I absorption toward the red limit. *Sci Adv* 2026;**12**:eaed7355. https://doi.org/10.1126/sciadv.aed7355

O'Malley-James JT, Kaltenegger L. UV surface habitability of the TRAPPIST-1 system. *Mon Not R Astronom Soc Lett* 2017;**469**:L26–30. https://doi.org/10.1093/mnrasl/slx047

O'Malley-James JT, Kaltenegger L. The vegetation red edge biosignature through time on earth and exoplanets. *Astrobiology* 2018;**18**:1123–36. https://doi.org/10.1089/ast.2017.1798

Pecaut MJ, Mamajek EE. Intrinsic colors, temperatures, and bolometric corrections of pre-main-sequence stars. *ApJS* 2013;**208**:9. https://doi.org/10.1088/0067-0049/208/1/9

Ritchie RJ, Larkum AWD, Ribas I. Could photosynthesis function on Proxima Centauri b? *Int J Astrobiol* 2018;**17**:147–76. https://doi.org/10.1017/S1473550417000167

Ritchie RJ. Consistent Sets of Spectrophotometric chlorophyll equations for acetone, methanol and ethanol solvents. *Photosynth Res* 2006;**89**:27–41. https://doi.org/10.1007/s11120-006-9065-9

Sagan C, Thompson WR, Carlson R. *et al.* A search for life on Earth from the Galileo spacecraft. *Nature* 1993;**365**:715–21. https://doi.org/10.1038/365715a0

Sanfilippo JE, Garczarek L, Partensky F. *et al.* Chromatic acclimation in cyanobacteria: a diverse and widespread process for optimizing photosynthesis. *Annu Rev Microbiol* 2019;**73**:407–33. https://doi.org/10.1146/annurev-micro-020518-115738

Schwieterman EW, Kiang NY, Parenteau MN *et al.* Exoplanet Biosignatures: a review of remotely detectable signs of life. *Astrobiology* 2018;**18**:663–708. https://doi.org/10.1089/ast.2017.1729

Shibata K., Spectrophotometry of translucent biological materials—opal glass transmission method. In Glick D. (Ed.), *Methods of Biochemical Analysis*, 1st edn, Vol. **7**, Wiley, 1959, 77–109. https://doi.org/10.1002/9780470110232.ch3

Shields AL, Ballard S, Johnson JA. The habitability of planets orbiting M-dwarf stars. *Phys Rep* 2016;**663**:1–38. https://doi.org/10.1016/j.physrep.2016.10.003

Swingley WD, Hohmann-Marriott MF, Le Olson T *et al.* Effect of iron on growth and ultrastructure of *Acaryochloris marina*. *Appl Environ Microb* 2005;**71**:8606–10. https://doi.org/10.1128/AEM.71.12.8606-8610.2005

Takizawa K, Minagawa J, Tamura M. *et al.* Red-edge position of habitable exoplanets around M-dwarfs. *Sci Rep* 2017;**7**:7561. https://doi.org/10.1038/s41598-017-07948-5

Tinetti G, Drossart P, Eccleston P. *et al.* A chemical survey of exoplanets with ARIEL. *Exp Astron* 2018;**46**:135–209. https://doi.org/10.1007/s10686-018-9598-x.

Tinetti G, Rashby S, Yung YL. Detectability of red-edge-shifted vegetation on terrestrial planets orbiting M stars. *Astrophys J* 2006;**644**:L129–32. https://doi.org/10.1086/505746

Trainer MG, Pavlov AA, DeWitt HL *et al.* Organic haze on Titan and the early Earth. *Proc Natl Acad Sci USA* 2006;**103**:18035–42. https://doi.org/10.1073/pnas.0608561103

Tucker CJ, Townshend JRG, Goff TE. African land-cover classification using satellite data. *Science* 1985;**227**:369–75. https://doi.org/10.1126/science.227.4685.369

Turnbull MC, Traub WA, Jucks KW *et al.* Spectrum of a habitable world: earthshine in the near-infrared. *Astrophys J* 2006;**644**:551–9. https://doi.org/10.1086/503322

Ulrich NJ, Shen G, Bryant DA *et al.* Ecological diversification of a cyanobacterium through divergence of its novel chlorophyll d-based light-harvesting system. *Curr Biol* 2024;**34**:2972–9. https://doi.org/10.1016/j.cub.2024.05.022

Viola S, Roseby W, Santabarbara S *et al.* Impact of energy limitations on function and resilience in long-wavelength Photosystem II. *eLife* 2022;**11**:e79890. https://doi.org/10.7554/eLife.79890

Wolf BM, Blankenship RE. Far-red light acclimation in diverse oxygenic photosynthetic organisms. *Photosynth Res* 2019;**142**:349–59. https://doi.org/10.1007/s11120-019-00653-6

Wolstencroft RD, Raven JA. Photosynthesis: likelihood of occurrence and possibility of detection on Earth-like Planets. *Icarus* 2002;**157**:535–48. https://doi.org/10.1006/icar.2002.6854

Zhen S. Substituting far-red for traditionally defined photosynthetic photons results in equal canopy quantum yield for CO_2 fixation and increased photon capture during long-term studies: implications for re-defining PAR. *Front Plant Sci* 2020;**11**:581156. https://doi.org/10.3389/fpls.2020.581156

Received: 10 April 2026. **Revised:** 26 June 2026. **Accepted:** 7 July 2026